MRI-tracking of transplanted human ASC in a SCID mouse model

Birte J. Siegmund[a], Annika Kasten[a], Jens-Peter Kühn[b], Karsten Winter[c], Cordula Grüttner[d], Bernhard Frerich[a,*]

[a] Department of Oral and Maxillofacial Surgery, Facial Plastic Surgery, Rostock University Medical Center, Germany
[b] Institute of Diagnostic Radiology and Neuroradiology, Greifswald University Medical Center, Germany
[c] Institute of Anatomy, Faculty of Medicine, University of Leipzig, Germany
[d] Micromod Partikeltechnologie GmbH, Rostock, Germany

ABSTRACT

Background: Regarding strategies improving the efficacy of stem cell transplantation in adipose tissue engineering, cell tracking might be useful. Here we report the *in vivo* tracking of adipose tissue derived stem cells (ASC) by means of nanoparticle labeling and magnetic resonance imaging (MRI). Here we report the *in vivo* tracking of adipose tissue derived stromal cells (ASC) by means of nanoparticle labeling and magnetic resonance imaging (MRI).
Materials and methods: Human ASC were amplified and labeled with two types of magnetic nanoparticles (MNP), BNF starch and nanomag®-D-spio. Adipose tissue constructs were fabricated by seeding collagen scaffolds with labeled and unlabeled ASCs. Constructs were implanted subcutaneously in the back of severe combined immunodeficient (SCID) mice (n =69, group 1: control with cells w/o label, group 2: BNF starch labeled cells, group 3: nanomag®-D-spio labeled cells). MRI scans were performed at 24 hours, four, twelve and 28 days and four months in a 7.1 T animal device. Explanted constructs were analyzed histomorphometrically.
Results: MRI scans showed high contrast of the labeled cells in t2-tse-sequence compared to unlabeled controls. Loss of volume of the implants was observed over time due to partial loss for transplanted cells without significant difference (level of significance $p < 0.017$). Compared to histomorphometry, there was found a positiv correlations in measurement of implant size with a significant at day four (correlation coefficient =0.643; p=0.024) and day twelve (correlation coefficient =0.687; p=0.010).
Additional Prussian blue stain showed iron in all implants. Significant differences between the three groups (significance level $p < 0.017$) were found after twelve days between control group and group 3 (p=0.008) and after 28 days between control group and group 2 and 3 (p=0.011).
Conclusion: Both MNPs might be suitable for tracking of ASC *in vivo* and show long term stability over 4 months.

1. Introduction

Soft tissue repair and augmentation is needed in many instances of plastic reconstructive and esthetic surgery. Current techniques of adipose tissue replacement are hampered by numerous drawbacks, as for example free lipotransfer lacks volume maintenance and implantation of synthetic materials may cause scarring or foreign body reactions [1,2]. Adipose tissue engineering using autologous adipose derived mesenchymal stem cells has been advocated as a solution [3–5]. However, current approaches for adipose tissue engineering likewise are lacking volume maintenance and form stability do to loss of transplanted cells and limitations in cell transplant efficiency. Insufficiency in nutritional supply is caused by failed connection to the host vasculature during the first time after transplantation and limits the efficiency of any kind of tissue or cells in order to develop improved strategies for cell transplantation, tools for visualization and tracking of transplanted cells *in vivo* are mandatory. A potential approach for visualization may be the labeling with magnetic nanoparticles (MNP) using magnetic resonance imaging (MRI) which is a current object of research in the field of cell based therapy.

In previous *in vitro* studies two types of MNP (bionized nanoferrite starch nanoparticles and superparamagnetic dextran coated iron oxide nanoparticles) had been proven suitability for visualization of adipose tissue derived mesenchymal stem cells in MRI. In conventional cell culture as well as in 3 D phantoms. [6,7]. Moreover, nanoparticle loading of ASC revealed no negative influence on proliferation and

differentiation, especially adipogenic differentiation of adipose tissue derived stem cells, when applied in the designated concentrations *in vitro*. BNF starch 10 µg Fe/ml and nanomag®-ᴅ-spio 25 µg Fe/ml had been proven to exert minimal detrimental effects, neither on proliferation nor on adipogenic differentiation. Already published data showed two examples of MNP loaded implanted cell scaffolds in MRI providing the feasibility of MNPs for cell visualization in MRI under *in vivo* conditions in general. In a second step, we report now the tracking of cell-loaded scaffolds after implantation *in vivo* in severe combined immunodeficient SCID mice in order to test the suitability of both nanoparticle types as intracellular contrast agents with a long term stability of several months. The implantation of human ASC into SCID mice is already approved as a study model [3]. Genetic mutation results in absence of b- and t-lymphocytes and natural killer cells [8].

The aim of this study was to prove the contrasting effect of transplanted human cells labeled by MNP in a SCID mouse model over time regarding cell degradation or signs of rejection. The results of MRI examination were compared to conventional histomorphometric slides. The major objective of this pilot study was to test the feasibility of both magnetic nanoparticle types for cell visualization *in vivo*. Should this technique turns out to be successful, the number of experimental animals in further studies could be reduced.

2. Material and methods

2.1. Cell cultivation, cell labeling and cultivation on collagenous scaffolds

Adipose tissue derived stem cells (ASC) were isolated from human adipose donor tissue. A small sample was taken from the subcutaneous fat of the iliac region during elective surgery. The study was approved by the Ethic Committee of the Rostock University Medical Center.

The adipose tissue was processed as described as published previously under sterile conditions [3,9,10]. The adipose tissue sample was minced with scissors and digested with collagenase NB 4 (Serva Electrophoresis GmbH, Heidelberg) at 37 °C. After centrifugation (10 min, 1300 rpm) and filtration, the pellet was resuspended in culture medium (Iscove´s modified Dulbecco's medium and Ham F12 1:1, both from Life Technologies GmbH, Darmstadt, Germany), supplemented with 10% newborn calf serum (NCS; PAA Laboratories, Pasching, Germany) and 1% penicillin-streptomycin (Life Technologies GmbH). The suspended cells were plated in tissue culture flasks (25 cm^2, Cellstar®, Greiner Bio-One, Frickenhausen, Germany). Cells were cultured in humidified 5% CO_2 atmosphere at 37 °C. The culture medium was changed every second day.

Cells were labeled with nanoparticles during the second and third passage with two types of magnetic iron oxid nanoparticles which both were provided by Micromod Partikeltechnologie GmbH, Rostock, Germany. On the one hand bionized nanoferrite starch particles (BNF starch) and on the other hand nanoferrite particles in a coat of dextran (nanomag®-ᴅ-spio) were applied, both particle types with a diameter of 100 nm. The characteristics and architecture of the nanoparticles have been reported elsewhere [11]. Details of the nanoparticle loading of ASC have been described and major effects on proliferation and differentiation could be excluded *in vitro* [7].

BNF starch and nanomag®-ᴅ-spio were applied at concentrations of 10 µg Fe/ml and 25 µg Fe/ml, respectively.

Both nanoparticle types were coated with poly-ᴅ-lysine (PDL; Sigma-Aldrich Chemie GmbH, Munich, Germany) to improve the intracellular particle uptake. Briefly, nanoparticles were treated with a solution of PDL in phosphate buffered saline (PBS; Sigma-Aldrich Chemie GmbH) (pH=7.4) with a concentration of 1.5 mg Fe/ml and 15 µg PDL/ml [6,12].

Afterwards, ASC were incubated with diluted MNP in culture medium according the previously described protocols. Collagen scaffolds (Medical Biomaterial Products MBP GmbH, Neustadt-Glewe,

Germany) were sterilized by steam autoclaving with formaldehyde gas (60–75 °C, 90 min) to increase the collagen cross-linking. Thereafter, scaffolds were soaked in 10% NCS/PBS. A formaldehyde test (Merck Darmstadt, Germany) was performed to exclude any residues. Labeled as well as unlabeled ASC were seeded on collagen scaffolds (1×2×0.5 cm) with a cell density of 1.5 million per scaffold. Scaffolds were kept in culture medium for additional three days in order to await attachment of the cells.

2.2. Animal experiments

Animal experiments were approved by the Local Comittee of Ethics of Animal Welfare (7221.3-1.1-039/12). Female severe combined immunodeficient mice of type beige (CB17. CG.*Prkdc^{scid}Lyst^{bg}/Crl*) with an age of 5 - 8 weeks and a weight of 14–22 g were obtained from Charles River Laboratories (Sulzfeld, Germany) (n=69). Three experimental groups were formed for the following experiments: group 1: control group with ASC scaffolds without labeling (n=19), group 2: ASC seeded scaffolds with BNF starch particle labeling (n=25), group 3: ASC seeded scaffolds with nanomag®-ᴅ-spio-particles (n=25).

MR-Scans were planned after 24 h (n=9), four days (n=12), twelve days (n=16), 28 days (n=16) and four months (n=16) in a 7.1 T small animal MRI (Table 1).

The operations were performed under sterile conditions under laminar air flow in an environment close to specific pathogen free conditions. Animals were anesthetized by intraperitoneal injection of Rompun® (Bayer Vital GmbH, Leverkusen, Germany) and Ketamine (Bela-pharm GmbH & Co. KG, Vechta, Germany). Dosage was adapted to body weight (b.w.) (0.016 mg/g b. w./0.12 mg/g b.w).

The cell seeded scaffolds were implanted subcutaneously at the back of the SCID mice using ceramic instruments in order to avoid metal artifacts in MRI.

An incision was made at the back by using a ceramic scalpel at the lateral on the right side of the spine, after subcutaneous preparation the scaffolds were brought into the wound cavity in the level between muscle layer and subcutis. Wounds were closed with single-button sutures using absorbable suture material (Resolon 5-0, Resorba Medical GmbH, Nürnberg, Germany). Postoperatively, mice were kept in groups of 4–6 per cage and fed with ssniff® V 1534-000 (10 mm pellets, ssniff Spezialdiäten GmbH, Soest, Germany) and water ad libitum.

For MRI examination, SCID mice were anesthetized with 4% isoflurane inhalation. During examination respiratory frequency and heart rate were monitored to adjust the depth of anesthesia.

T2-weighted sequence was used to visualize and to assess the distribution of ASC *in vivo* labeled with nanoparticles. Coronal T2-weighted turbo spin echo MRI was performed and sequence was acquired using the following image parameters: TR: 1300 ms; TE: 43 ms; flip angle: 1801; matrix: 320×240; field of view: 41 mm; 1 averages: 1, bandwidth 130 Hz, slice thickness: 0.7 mm. Image analysis was performed using the freeware Osirix (Version 5.6, Pixmeo, Bernex,

Table 1
grouping of animals; h=hours, d=days, mo=months.

time point of postoperative MRI	group 1: ASC Scaffolds without labeling	group 2: ASC-Scaffolds +BNF-Starch	group 3: ASC-Scaffolds +nanomag®-ᴅ-Spio	total
24 h	3	3	3	9
4 d	4	4	4	12
12 d	4	6	6	16
28 d	4	6	6	16
4 mo	4	6	6	16
total	19	25	25	69
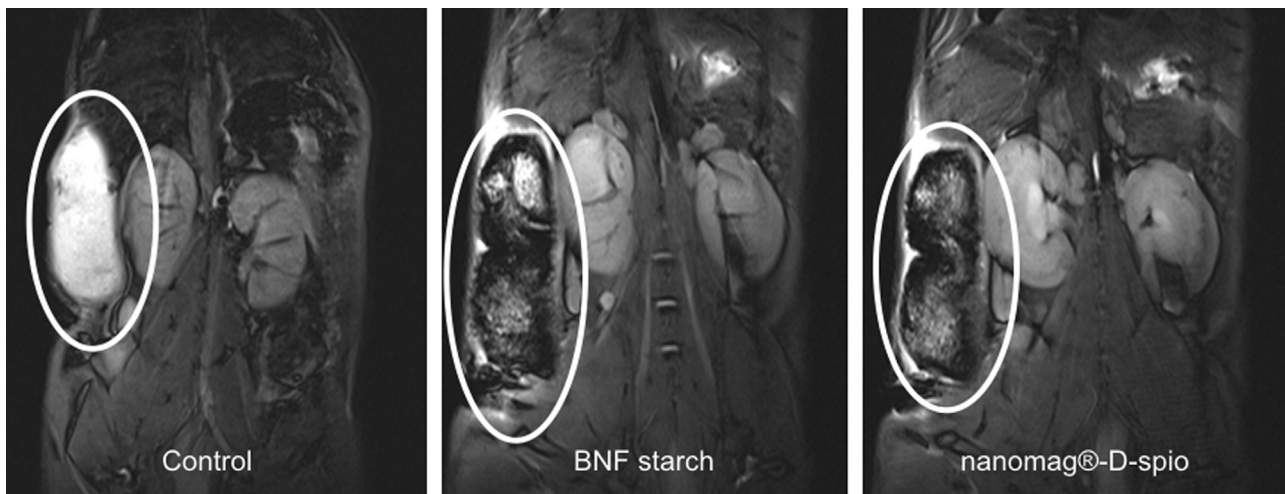
Fig. 1. MRI scans (t2-tse-sequence, coronary view), four days after implantation. The implanted scaffolds are marked with an ellipse. Control group shows collagenous scaffolds with unlabeled ASC, BNF starch and nanomag®-ᴅ-spio labeled cells showed high contrast on the collagenous scaffolds.
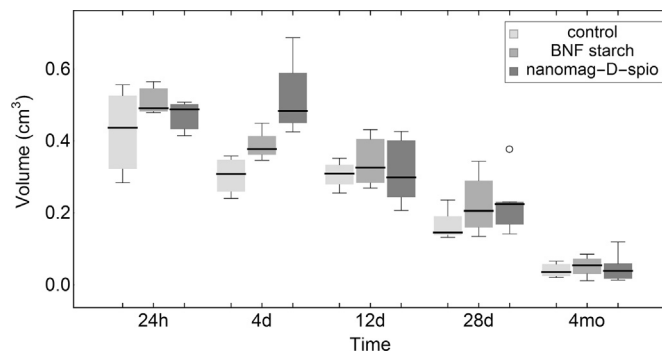
Fig. 2. Decreasing volume of the cell seeded constructs in all groups between 24 h and four months after implantation (group 1: control group with ASC seeded scaffolds without nanoparticle labeling, group 2: BNF starch loaded ASC-scaffolds (10 µg Fe/ml) and group 3: nanomag®-ᴅ-spio loaded ASC-scaffolds (25 µg Fe/ml). The outlier value in group 3 at 28 days p.o. can be explained by artifacts in the t2-tse-sequence leading to measurement inaccuracy.

Switzerland). Manual segmentation of cell-seeded collagen scaffolds was done in each slice in the coronary view using the region of interest tool. After segmentation, the volume of each scaffold was calculated as a 3 D reconstruction. In addition, a subjective image analysis was performed to assess the distribution of nanoparticle-labeled cells.

2.3. Histomorphometric analysis

SCID mice were sacrificed immediately after MRI examination. Constructs were explanted and fixed with 4% formaldehyde buffered in saline at pH 7.4 (Formafix, Grimm med Logistik GmbH, Torgelow, Germany). Specimens were embedded in paraffin and histologically sectioned along the long axis. Sections were stained with hematoxylin eosin. Implant cross sectional area was measured by using the specimen with the largest diameter in the center of the implant. A second series of sections was stained with prussian blue stain in order to visualize MNP, counterstaining was performed with nuclear fast red. Stained specimen were scanned in a MIRAX MIDI digitizer (Carl Zeiss Microscopy GmbH, Jena, Germany). Histomorphometrical analysis was performed with AxioVision software version 4.8.2 (Carl Zeiss Microscopy GmbH, Jena, Germany).

2.4. Statistical analysis

Statistical analysis was performed using IBM SPSS Statistics (version 22; IBM Corp.; Armonk, New York, USA). Correlation was
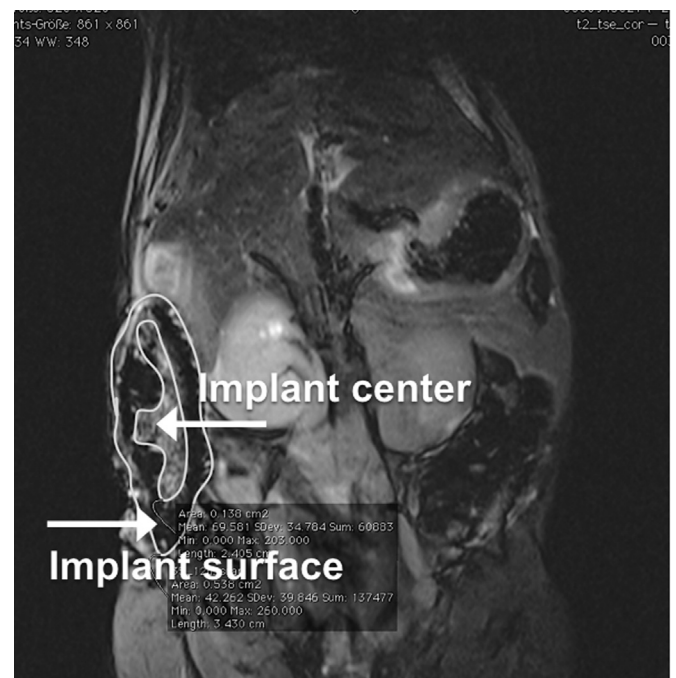
Fig. 3. MRI scan (t2-tse-sequence, coronary view), twelve days after implantation of ASC-scaffold loaded with nanomag®-ᴅ-spio-particles. The picture shows an outer layer with high concentration of MNP. The signal is hypointense because of the susceptibility effect of the iron oxide. The transplant center appears hyperintense because of low concentration of iron oxide.

computed using bivariate correlation analysis with Spearman correlation coefficient (-1, 0 and 1 representing total negative correlation, no correlation and total positive correlation, respectively) and 2-tailed significance. Data was tested for normal distribution using the Shapiro-Wilk test. Group comparisons were performed using Kruskal-Wallis and Mann-Whitney-U tests. Significance was set at $p < 0.05$. Bonferroni correction was used to adjust the p-value.

3. Results

Of the total amount of 69 animals, six mice had to be excluded from further analysis due to perioperative complications like bacterial wound infection or death ahead of schedule. The other animals showed no signs of infection or other complications. All mice showed gain in weight, no significant difference between the groups were observed.
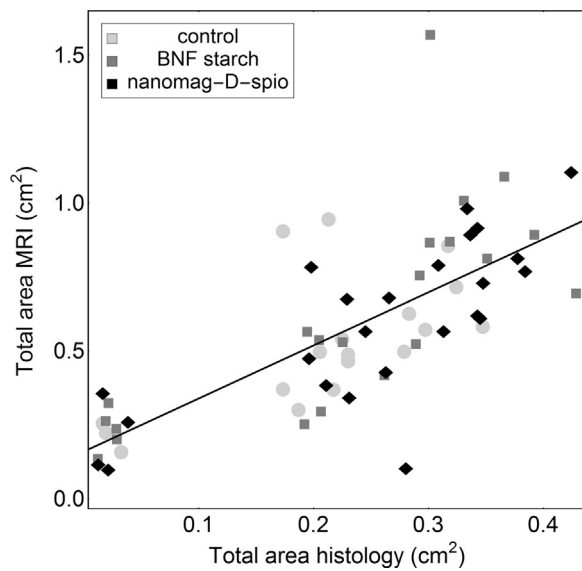
Fig. 4. Correlation between implant diameters (cm ^{2}) in MRI and histomorphometry. A positive correlation is shown with a significance at day four (correlation coefficient=0.643; p=0.024) and day twelve (correlation coefficient=0.687; p=0.010).

3.1. MRI

Detection of implanted cell constructs in the nanoparticle labeled groups was successful to all time points. Due to the susceptibility effect of the iron oxide, MNP loaded cell scaffolds showed a clear contrast to the hyperintense environment, which could be measured in the t2-tse-sequence. In this way, cell detection was possible up to four months. Because of the susceptibility effect of the iron oxide, MNP loaded cells caused a signal loss in MRI. Cells were shown hypointense und could be easily distinguished from the surrounding environment. The implanted scaffolds of the control group showed no contrast, no cell formation was found on the hyperintens collagenous scaffold (Fig. 1).

Volume measurement in MRI showed a similar loss of volume of the constructs in all groups. Statistical analysis did not show any significance in group comparison between control group, group 2 (BNF starch) and group 3 (nanomag®-D-spio)$_D$ (p < 0.017) (Fig. 2).

MNP loaded cells were successfully shown in MRI, compared to the control group were cells were invisible. Particle distribution was localized inhomogeneous in order to cell arrangement and cell seeding method. As a result, the expression of iron oxide in the outer layers was higher then in the implant center. However, an emigration of cells or rather of MNPs was observed over time in MRI scans inside the implants what makes this method suitable to show results of dynamic processes like tracking of cells *in vivo* in a longitudinal study design. Over time, the expression of an outer zone with high iron oxide concentration and an center with low iron concentration, especially

at day twelve and day 28 after implantation was observed (Fig. 3).

Because of almost total decrease of implants after four months, a division in zones with high and low iron density could not be made in MRI nor under microscope. The ratio of the outer zone with high iron oxide content and the center of the construct did not show a significant difference regarding both MNP. The outer zone with high MNP labeled cells was growing in relation to the implant center with a lack of vascularization.

Iron concentration could be measured by using the r2* weighted sequence. A positive signal could be measured in rough data. However, a quantification of by using the r2* sequence between 24 h and four months was not possible under *in vivo* conditions because of partially high iron concentrations inside the implants, which leaded to immeasurable high values. An estimation of cell concentration by quantifying iron oxide was difficult in this experimental set up.

3.2. Histomorphometry

Histomorphometric analysis showed a shrinking of the implants over a time of four months. Analogous to volume analysis in MRI, no significant difference was found between control group, group 2 (BNF starch) and group 3 (nanomag®-D-spio) (p < 0.017).

Both methods, the measurement of the transplant diameters in MRI and in histomorphometry, showed a positive correlation with a significance at day four (correlation coefficient=0.643; p=0.024) and day twelve (correlation coefficient=0.687; p=0.010) (Fig. 4).

Furthermore, MNP were successfully shown inside the transplanted stem cells using prussian blue stain. Control groups showed iron containing cells in prussian blue stain too, in contrast to the MRI-Scans, where no iron oxide was measured in the t2-tse-sequence. The reason for that is the infiltration of inflammatory cells from the host organism in context wound healing like macrophages resorbing the postoperative hematoma. A significant difference between control group and particle labeled groups was measured only at day twelve between control and nanomag®-D-spio (p=0.008) and between both particle labeled groups and control group at day 28 (p=0.011).

4. Discussion

In the already published data, MNP were tested under *in vitro* conditions for ASC labeling and cell tracking in MRI using cell-agarose-phantoms. Material characteristics and influences on cell viability, cell proliferation and cell differentiation was examined in cell culture.

Following these previous *in vitro* studies and based on these results, cell tracking in MRI using MNP was successful in a 7.1 T MRI using a t2 weighted sequence. Cells were visualized indirectly by the susceptibility effect of the iron oxide in the MNP labeled groups, making this method suitable for cell tracking *in vivo* up to four months. So far, MNP labeling is able to replace histomorphometric measurements and therefore can help sparing animals. Long term stability and
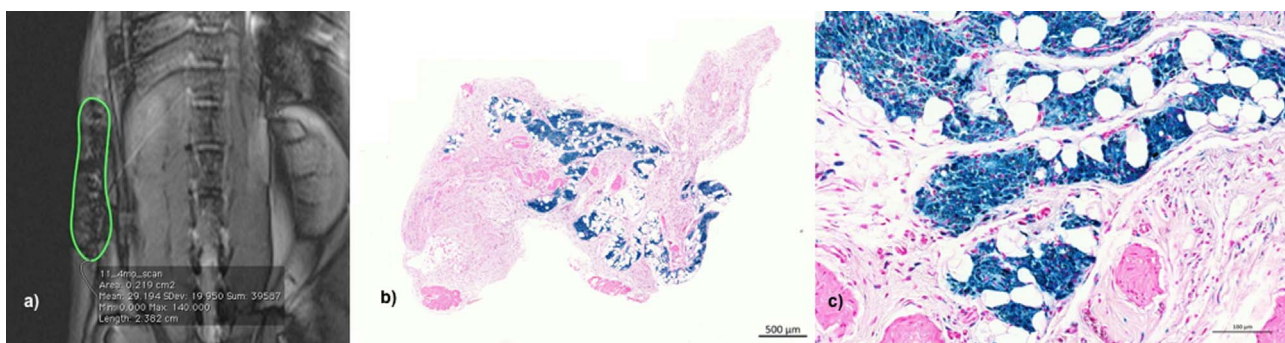
Fig. 5. MRI scan (t2-tse-cor) of the BNF starch labeled groups four months after implantation (a) with the corresponding specimen (b) (Prussian blue/nuclear fast red stain (1:10)) with enlarged view (c).

high resolution make MNP labeling for cell tracking in MRI suitable for longitudinal study concepts [13–19].

T2 weighted sequence was used for cell imaging. Compared to previous *in vitro* studies, a quantification of the transplanted cells was difficult *in vivo* in using the r2*-sequence [20], because of irregular cell and particle distribution on the collagenous scaffolds. Dynamic processes in the living organsim leaded to a cell migration over time after implantation. A lack of blood supply especially in the implant center caused cell or rather MNP migration to the implant surface, which was observed as well as an immigration of cells from the host environment into the constructs.

A differentiation between an outer layer with a zone of cell proliferation and an implant center with low density was observed twelve days and also 28 days after post implantation in MRI as well as in histomorphometry, but without a specific correlation in statistical analysis due to large variance within the experimental groups.

Nevertheless, MRI tracking of implanted cells by labeling with MNP is an indirect method of cell visualization, information about cell vitality cannot be made by using this method. Shrinkage of volume and resorption of the implants was expected because of collagen resorption as the result of enzymatic degradation [21] and low cell density on the cell scaffolds. Clinical signs of a rejection reaction or incompatibility were not observed. After four months, the tissue engineered constructs were considerably shrunken. MNP could still be detected in the area of the scare tissue in MRI (Fig. 5).

Prussian blue stain was successful for detecting iron oxide inside the implants and also in the environmental area of the implant and emigrated cells from the host organism. Because of the unspecific staining of iron containing structures, the detection of MNPs was difficult and not possible without artifacts. If required, another method for detecting MNPs in histomorphometric analysis might be preferred in future experimental setups.

The main focus of this study was the visualization of cells at different time points after implantation. Both MNP, BNF starch and nanomag®-D-spio, showed high contrast in the used concentrations with a long term stability of four months. Clinical signs of incompatibility could not be obserserved. Based on the results of this pilot study, improvement of cell survival, proliferation and differentiation of the cells *in vivo* can be the next stage.

5. Conclusion

Both types of nanoparticles, BNF starch and nanomag®-D-spio, enable labeling of ASC and visualization of cell loaded scaffolds in MRI with high contrast. Furthermore, labeling remained stable over a period of 4 months. Labeled cells were successfully visualized *in vivo* after transplantation and could be distinguished from the surrounding tissue as well as the collagen scaffold. In the unlabeled control group, cells and collagen scaffold showed a homogenous signal and could not be distinguished. Even in stage of full resorption of the implants, cells could be detected by the MNP within the scar tissue. However, cell tracking by MNP is an indirect method for cell tracking, a differentiation between vital and avital cells is not possible. Now, further studies are necessary to establish this method in experimental research and enable the quantification of iron using MRI by reducing nanoparticle concentrations for cell labeling.

Acknowledgements

References

[1] R.D. Largo, L.A.H. Tchang, V. Mele, A. Scherberich, Y. Harder, R. Wettstein, D.J. Schaefer, Efficacy, safety and complications of autologous fat grating to healthy breast tissue: a systemic review, J. Plast., Reconstr. Aesthet. Surg. 67 (2014) 437–448.

[2] U. Wollina, A. Goldman, Dermal fillers: facts and controversies, Clin. Dermatol. 31 (2013) 731–736.

[3] B. Frerich, K. Winter, K. Scheller, U.-D. Braumann, Comparison of different fabrication techniques for human adipose tissue engineering in severe combined immunodeficient mice, Artif. Organs 36 (2012) 227–237.

[4] R. Kosaraju, R.C. Rennert, Z.N. Mann, D. Duscher, J. Barrera, A.J. Whittam, M. Januszyk, J. Raiadas, M. Rodrigues, G.C. Gurtner, Adipose-derived stem cell-seeded hydrogels increase endogenous progenitor cell recruitment and neovascularization in wounds, Tissue Eng. Part A 22 (2016) 295–305.

[5] N.M. Toyserkani, M.L. Quaade, J.A. Sorensen, Cell-assisted lipotransfer: a systematic review of its efficacy, Aesthet. plast. surg. 40 (2016) 309–318.

[6] A. Kasten, C. Grüttner, J.P. Kuhn, R. Bader, J. Pasold, B. Frerich, Comparative in vitro study on magnetic iron oxide nanoparticles for MRI tracking of adipose tissue-derived progenitor cells, PLoS One (9) (2014) e108055.

[7] A. Kasten A, B.J. Siegmund, C. Grüttner, J.-P. Kühn, B. Frerich, Tracking of adipose tissue-derived progenitor cells using two magnetic nanoparticle types, J. Magn. Magn. Mater. 380 (2015) 34–38.

[8] J.P. Sundberg, Handbook of Mouse Mutations with Skin and Hair Abnormalities. Animal Models and Biomedical Tools, CRC Press Inc., Boca Raton, 1994.

[9] B. Frerich, J. Kurtz-Hoffmann, N. Lindemann, S. Müller, Tissue engineering of vascularized bone and soft tissue transplants, Mund Kiefer Gesichtschir. 4 (2) (2000) 490–495.

[10] B. Frerich, N. Lindemann, J. Kurtz-Hoffmann, K. Ortel, In vitro model of a vascular stroma for the engineering of vascularized tissues, Int. J. Oral. Maxillofac. Surg. 30 (2001) 414–420.

[11] D.E. Bordelon, C. Cornejo, C. Grüttner, F. Westphal, L. DeWeese, R. Ivkov, Magnetic nanoparticle heating efficiency reveals magneto-structural differences when characterized with wide ranging and high amplitude alternating magnetic fields, J. Appl. Phys. 109 (2011) 124904-0–124904-8.

[12] M. Hedayati, O. Thomas, B. Abubaker-Sharif, H. Zhou, C. Cornejo, The effect of cell cluster size on intracellular nanoparticle-mediated hyperthermia: is ist possible to treat microscopic tumors?, Nanomed. (Lond.) 8 (2013) 29–41.

[13] E. Küstermann, U. Himmelreich, K. Kandal, T. Geelen, A. Ketkar, D. Wiedermann, C. Strecker, J. Esser, S. Arnold, M. Hoehn, Efficient stem cell labeling for MRI studies, Contrast Media Mol. Imaging 3 (2008) 27–37.

[14] U. Himmelreich, T. Dresselaers, Cell labeling and tracking for experimental models using magnetic resonance imaging, Methods 48 (2009) 12–124.

[15] W. Liu, J.A. Frank, Detection and quantification of magnetically labeled cells by cellular MRI, Eur. J. Radiol. 70 (2009) 258–264.

[16] N. Muja, J.W.M. Bulte, Magnetic resonance imaging of cells in experimental disease models, Prog. Nucl. Magn. Reson. Spectrosc. 55 (2009) 61–77.

[17] B. Addicott, M. Willman, J. Rodriguez, K. Padgett, D. Han, D. Berman, J.M. Hare, N.S. Kenyon, Mesenchymal stem cell labeling and in vitro MR characterization at 1.5 T of new SPIO contrast agent: molday ION rhodamine-b, Contrast Media Mol. Imaging 6 (2010) 7–18.

[18] C. Lalande, S. Miraux, S.M. Derkaoui, S. Mornet, R. Bareille, J.C. Fricain, J.M. Franconi, C. Le Visage, D. Letourneur, J. Amédée, A.K. Bouzier-Sore, Magnetic resonance imaging tracking of human adipose derived stromal cells within threee-dimensional scaffolds for bone tissue engineering, Eur. Cells Mater. 21 (2011) 341–354.

[19] T. Struys, A. Ketkar-Atre, P. Gervois, C. Leten, P. Hilkens, W. Martens, A. Bronckaers, T. Dresselaers, C. Poliits, I. Mabrichts, U. Himmelreich, Magnetic resonance imaging of human dental pulp stem cells in vitro and in vivo, Cell Transplant. 22 (2013) 1813–1829.

[20] J.-P. Kuehn, D. Hernando, A.M. del Rio, M. Evert, S. Kannengiesser, H. Völzke, B. Mensel, R. Puls, N. Hosten, S.B. Reeder, Effect of multipeak spectral modeling of fat for liver iron and fat quantification: correlation of biopsy with MR imaging results, Radiology 265 (2012) 133–142.

[21] P.B. Malafaya, G.A. Silva, R.L. Reis, Natural–origin polymers as carriers and scaffolds for biomolecules and cell delivery in tissue engineering applications, Adv. Drug Deliv. Rev. 59 (2007) 207–233.